

Characterization of porous core layer for controlling rare earth incorporation in optical fiber

Anirban Dhar, Mukul Ch. Paul, Mrinmay Pal, Ashok Kr. Mondal, Suchitra Sen, Himadri Sekhar Maiti, Ranjan Sen

*Fiber Optics Laboratory, Central Glass & Ceramic Research Institute,
196, Raja S.C. Mullick Road, Kolkata, India.
rsen@cgcri.res.in*

Abstract: The porous core layer deposited by modified chemical vapour deposition process has been analyzed in terms of thickness, pore size distribution, homogeneity and characteristics of the soot particles to investigate their variation with deposition temperature and input vapour composition. The compositions selected were SiO₂, SiO₂-GeO₂ and SiO₂-P₂O₅. Rare earth ions were incorporated into the deposit by a solution doping technique. The analysis of deposited microstructures was found to provide a quantitative indication about the rare earth incorporation and its variation with respect to process conditions. Thus the characterization provides a method of controlling rare earth doping and ultimate preform/fiber properties.

©2006 Optical Society of America

OCIS codes: (060.2280) Fiber design and fabrication; (060.2410) Fibers, erbium; (999.9999) solution doping technique; (999.9999) porous soot layer.

References and links

1. S. B. Poole, D. N. Payne, M. E. Fermann, and R. I. Laming, "Fabrication of low-loss optical fibers containing rare earth ions," *Electron. Lett.* **21**, 737-738 (1985).
2. J. E. Townsend, S. B. Poole, and D. N. Payne, "Solution doping technique for fabrication of rare-earth doped optical fibers," *Electron. Lett.* **23**, 329-331 (1987).
3. J. Stone and C. A. Burrus, "Nd³⁺ doped SiO₂ lasers in end pumped fiber geometry," *Appl. Phys. Lett.* **23**, 388-389 (1973).
4. V. Matejec, M. Hayer, M. Pospisilova, and I. Kasik, "Preparation of optical cores of silica optical fiber by the sol-gel method," *J. Sol-Gel Sci. Technol.* **8**, 889-893 (1997).
5. M. Rajala, K. Janka, S. Tammela, P. Stenius, P. Kiiveri, and M. Hotoleanu "Advantages of direct nanoparticle deposition (DND) technology in active fiber production" <http://www.lekki.fi/doc/Liekki%20white%20Paper-DNDFiberIntro-May2005.pdf>
6. M. Chatterjee, R. Sen, M. Pal, M. Naskar, M. Paul, S. Bhadra, K. Dasgupta, D. Ganguli, T. Bandyopadhyay, A. Gedanken, and R. Reisfeld, "Rare-earth doped optical fiber from oxide nanoparticle," *Acta. Opt. Sin.* **23**, 35-36 (2003).
7. Tingye Li, *Optical Fiber Communications, Vol. 1 on Fiber Fabrication* (Academic Press, 1985) Chap. 1.
8. B. J. Ainslie, "A Review of the fabrication and properties of erbium-doped fibers for optical amplifiers," *J. Lightwave Technol.* **9**, 220-227 (1991).
9. D. J. DiGiovanni, S. Plains, and K. L. Walker, US Patent "System comprising Er-doped optical fiber," No. 5,058,976, filed on August 3, 1990.
10. D. Tanaka, A. Wada, T. Sakai, T. Nozwa, and R. Yamauchi, US Patent "Solution doping of a silica preform with erbium, aluminium and phosphorus to form an optical fiber" No. 5,474,588, filed on September 16, 1994.
11. T. Bandyopadhyay, R. Sen, S. Kr. Bhadra, K. Dasgupta, and M. Ch. Paul, US Patent "Process for making rare earth doped optical fiber" No. 6,751,990, filed on March 6, 2001.
12. V. Matejec, I. Kasik, D. Berkova, M. Hayer, M. Chomat, Z. Berka, A. Langrova, J. Kanka, and P. Honzatko, "Properties of optical fiber preforms prepared by inner coating of substrate tubes," *Ceram. Silik.* **45**, 62-69 (2001).
13. Y. H. Kim, U. C. Paek, and W. T. Han, "Effect of soaking temperature on concentrations of rare-earth ions in optical fiber core in solution doping process," in *Rare-earth doped Materials and Devices*, V. Shubin Jiang, eds., Proc. SPIE **4282**, 123-132 (2001).

14. E. Potkay, H. R. Clark, I. P. Smith, T. Y. Kometani, and D. L. Wood, "Characterization of soot from multimode vapour phase axial deposition optical fiber preforms," *J. Lightwave Technol.* **6**, 1338-1347 (1988).
 15. S. S. Mukhopadhyay and D. Kundu, "Chemical composition analysis of Germanate glass by alkalimetric titration of Germinate Mannitol complex," *J. Indian Chemical Soc.* **83(3)**, 255-258 (2006).
 16. S. J. Gregg and K. S. W. Sing, *Adsorption, Surface Area and Porosity*, 2nd ed. (Academic Press, New York, 1982).
 17. M. Pal, R. Sen, M. C. Paul, S. K. Bhadra, S. Chatterjee, D. Ghosal, and K. Dasgupta "Investigation of the deposition of porous layers by the MCVD method for the preparation of rare-earth doped cores of optical fibers," *Opt. Commun.* **254**, 88-95 (2005).
 18. D. J. DiGiovanni, J. B. MacChesney, and T. Y. Kometani, "Structure and properties of silica containing aluminum and phosphorus near the AlPO_4 join," *J. Non-Cryst. Solids* **113**, 58-64 (1989).
-

1. Introduction

Optical fibers doped with rare earth (RE) ions have shown great promise for their application in the development of optical amplifiers, fiber lasers and sensors. There has been rapid progress in this field during the last few years. The increasing demand for the fibers led to intensive R&D effort to improve the fiber performance and produce the fibers more reproducibly. A number of techniques such as vapor phase doping [1], solution doping [2, 3], sol-gel dip-coating [4], direct nanoparticle deposition [5], dip coating using RE oxide coated nanoparticles [6] etc. have been developed to incorporate the RE ions in the core in specific proportion without formation of undesired clusters. Modified chemical vapor deposition (MCVD) [7] process coupled with solution doping technique is mostly used to fabricate the fiber, even for commercial production, because of its simplicity and flexibility in doping different REs in various concentrations. However, all the techniques have the inherent difficulty of maintaining proper control over the preform/fiber parameters such as RE concentration, compositional homogeneity, dopant distribution etc.

In the solution doping method the deposited porous core layer inside a silica tube is soaked into a solution containing salts of RE and co-dopants. A schematic diagram of the method is shown in Fig. 1. The critical step in this process is the deposition of a uniform soot layer of suitable composition and porosity which serves as a precursor for soaking desired amount of RE ion. The variation in porosity and density as well as the pore size distribution leads to poor control of RE concentration and inhomogeneity along the length of the preform and fiber. As a result, identical lengths of fiber do not provide the same performance. On the other hand the composition of the soaking solution, the Al/RE ratio, the nature of solvent, etc. are the controlling factors during the solution doping step to achieve the desired properties in the fiber. Although many investigations have been reported [8-13] on the influence of different doping parameters on the ultimate fiber properties, very few have concentrated on the porous soot layer characteristics which control the RE incorporation efficiency. Unless the soot layer morphology is completely known and can be controlled with respect to the fabrication conditions, the fiber performance cannot be improved. Some data have been reported on the soot characteristics of a multimode soot boule prepared by VAD process [14] but no such result is available for soot layers deposited by MCVD process.

The motivation of the present work lies on this background. The unsintered soot layer characteristics have been critically analyzed to investigate the influence of deposition temperature and composition on the porous deposit microstructures and consequent effect on the final preform/fiber properties with the rare earth ion incorporation in particular.

2. Experimental

The MCVD process was followed to deposit porous silicate layers of various compositions at selected temperatures inside a 20 mm diameter silica tube. The burner traverse speed was 12.5 cm/min during deposition and the flame width was 15 mm. The total flow through the tube was 0.6 liter/min at the input gas temperature of 25°C.

In the first series of experiment, we deposited porous core layers consisting of pure SiO_2 , $\text{SiO}_2+\text{GeO}_2$ ($\text{GeCl}_4/\text{SiCl}_4=0.86$) and $\text{SiO}_2+\text{P}_2\text{O}_5$ ($\text{POCl}_3/\text{SiCl}_4=0.48$) to study the compositional effect on soot layer morphology. A temperature in the range of 1200-1300°C was selected for depositing pure SiO_2 and $\text{SiO}_2+\text{GeO}_2$ layers. Since at this temperature $\text{SiO}_2+\text{P}_2\text{O}_5$ soot starts sintering, a number of experiments were carried out to find out a suitable temperature for depositing $\text{SiO}_2-\text{P}_2\text{O}_5$ compositions and ultimately this soot layer was deposited at around 1100°C. The other experimental conditions remained same for all compositions.

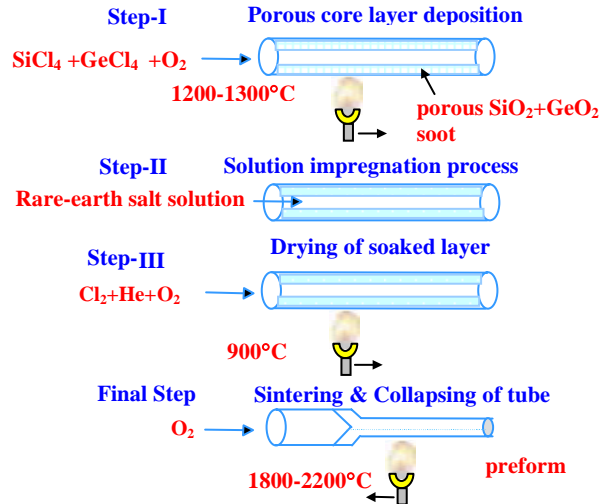


Fig. 1. Different steps of solution doping process.

In another series of experiment, GeO_2 doped core layers were deposited at temperatures of 1220, 1255 & 1295°C maintaining the same vapor phase composition ($\text{GeCl}_4/\text{SiCl}_4=0.86$) in order to study the influence of deposition temperature on the porous deposit characteristics as well as on the fabricated fiber in terms of rare earth ion concentration.

In both the above series of experiments, preforms and fibers were fabricated using a solution of 0.01 M $\text{ErCl}_3 + 0.3$ M AlCl_3 in ethanol. Problems of crack development in the soot deposit and disengagement from the tube surface occurred during solution doping of pure SiO_2 layer due to its poor adhesion with the tube surface. These preforms contained defects and were not used for drawing fibers. Subsequent to solution doping the soot deposit was oxidized and dehydrated. The dehydration was carried out by supplying Cl_2 at a temperature of 900°C. The layer was sintered in the presence of oxygen and helium at temperatures in the range 1400 to 1700°C. Collapsing was done at a higher temperature of about 2200°C to obtain the preform. Fibers of $125\pm 0.5\mu\text{m}$ diameter with dual resin coating were drawn from the preforms in a conventional tower (Heathway, UK make).

Scanning electron microscopy (SEM) of different soot layer samples were performed (using a LEO-430i) to investigate the change in the deposit microstructures and thickness with change in temperature as well as composition before solution doping. The analysis was repeated after solution doping to study the impregnation of dopants into the micropores. Field emission SEM (FESEM) was used for analyzing the porous network structure and morphology of individual pores. Image analysis (LEICA Q 500 MC) of the SEM micrographs was performed to analyze the pore size distribution. The compositions of the soot particles were determined using chemical analysis. A special analytical method using mannitol was developed for this purpose [15]. Mannitol, a polyhydric alcohol, formed germinate mannitol complex which was alkalimetrically titrated. The BET (Brunaur-Emmett-Teller) surface area of the soot samples collected from the deposit was evaluated by liquid N_2 adsorption method

[16]. The surface area provided an idea about the dimension of the pores formed by the structures.

Preforms prepared were characterized using PK2600 (Photon Kinetics, USA) preform analyzer to measure different optical and geometrical characteristics before drawing the fiber. Different fiber characteristics such as refractive index (RI) profile, numerical aperture (NA), core/clad geometry etc. were measured using an NR-20 fiber analyzer (EXFO, Canada) followed by spectral attenuation measurements using cutback method (Bentham, UK make instrument). The Er ion concentration in the core was determined from the 980 nm absorption peak in the attenuation curve. The radial concentration distributions of Er and Al were measured in a few preform samples by electron probe microanalysis (EPMA) and X-ray microprobe analysis.

3. Results and discussion

The SEM micrograph of a porous deposit on the inside surface of a silica tube is shown in Fig. 2. The photograph, taken in a transverse direction, demonstrates good homogeneity with minimum imperfection at the interface. The thickness of the deposited layer was found to be dependent upon deposition temperature and composition. The gradual addition of dopants such as GeO_2 and P_2O_5 led to decrease in the thickness compared to that of pure SiO_2 layer due to lowering of viscosity and sintering temperature, which results in densification of the layer. The thickness was minimum (mostly below $5\ \mu\text{m}$) for P-doped soot layer as P facilitates the sintering appreciably. In the case of the GeO_2 doped layer, the thickness varied from $3.5\ \mu\text{m}$ to $7.5\ \mu\text{m}$ when temperature was changed from 1295°C to 1255°C . The variation in thickness also appeared to be due to partial consolidation with rise in temperature. The deposited layer thickness is an important parameter to optimize the soaking time in the solution and also to achieve the appropriate core thickness in the ultimate fiber. A typical FESEM picture of the porous layer is shown in Fig. 3. The individual pores are clearly observed in the micrograph. Examination of the individual pore shows little imperfection at pore boundary, the average size of which is $1.5\ \mu\text{m}$ in diameter. The burned raster seen in the center of the Fig. 3 appeared as a result of beam impression due to long exposure during taking the micrograph.

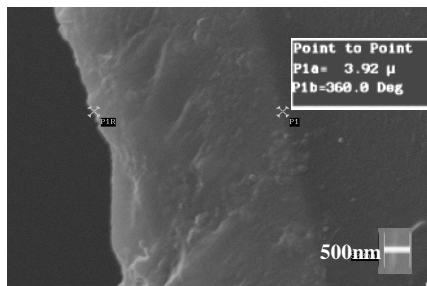


Fig. 2. SEM micrograph showing GeO_2 doped porous core layer deposited at 1295°C .

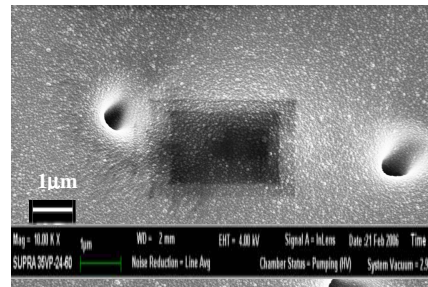


Fig. 3. FESEM micrograph showing the pores of GeO_2 doped soot deposited at 1295°C .

The SEM micrographs of GeO_2 doped soot layers deposited at temperatures of 1220° and 1295°C are shown in Figs. 4(a) and 4(b). Comparison of the said micrographs indicates that the network formation of the soot particles and the pore size distribution are strongly influenced by temperature. The image analysis of the micrographs provides a quantitative comparison. If the number of pores in the range $1\text{-}2\ \mu\text{m}$ is taken as an indicator of uniformity, then it is found that the uniformity of pore size distribution reduces from 70% to 59% corresponding to the above temperature increment. The curves (a) and (b) in Fig. 5 represent pore size analysis of the soot deposit at temperatures of 1295° and 1255° respectively. It is observed that the pore size has a wider distribution at higher temperature although the mean

pore size remains in the range of 1.5 μm . Thus at higher temperature the pores seem to collapse and also fuse together resulting in greater pore size variation and decrease in porosity due to partial consolidation. A pore area fraction, defined by the ratio of total pore area to the area of the deposit under consideration, showed a variation of 32% to 24% for increase in temperature from 1255° to 1295°C.

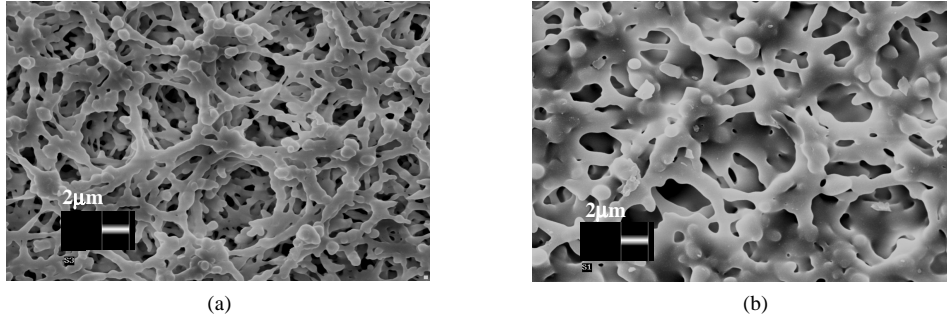


Fig. 4. SEM micrograph of $\text{SiO}_2\text{-GeO}_2$ soot deposited at temperature (a) 1220°C and (b) 1295°C.

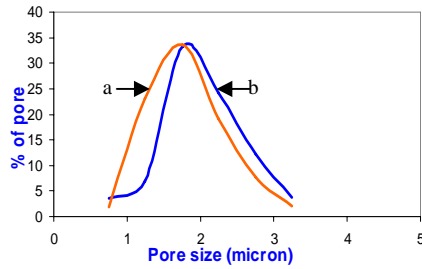


Fig. 5. Pore size distribution for $\text{SiO}_2\text{-GeO}_2$ against deposition temperature (a) 1295°C, (b) 1255°C.

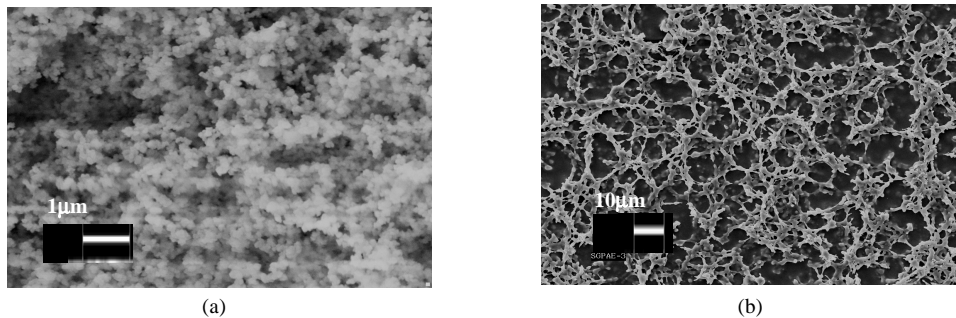


Fig. 6. SEM micrograph of (a) SiO_2 deposited at 1300°C and (b) $\text{SiO}_2\text{-P}_2\text{O}_5$ deposited at 1100°C.

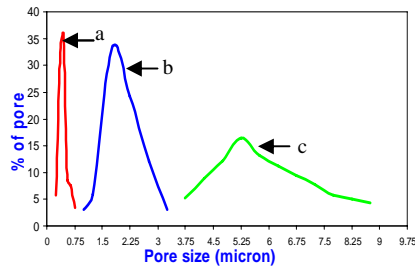


Fig. 7. Variation of pore size with composition (a) SiO_2 , (b) $\text{SiO}_2\text{+GeO}_2$, (c) $\text{SiO}_2\text{+P}_2\text{O}_5$.

The SEM micrographs presented in Fig. 6 show the change in porous layer morphology with change in composition. While pure SiO_2 deposit is homogeneous with finer network

structure, the $\text{SiO}_2+\text{P}_2\text{O}_5$ network is composed of pores with wide variation in shape and size. Such variation is a consequence of pore collapsing and combining together as P facilitates sintering at lower temperature. Further comparison with GeO_2 doped layer shown in Fig. 4 clarifies the difference in network structure for the three different compositions. The GeO_2 doped deposit has an intermediate structure between SiO_2 and $\text{SiO}_2+\text{P}_2\text{O}_5$ composition. Image analysis data in Fig. 7 presents the variation in pore size distribution in relation to soot composition. The mean pore size is found to be $0.5\ \mu\text{m}$ for SiO_2 , $1.5\ \mu\text{m}$ for $\text{SiO}_2+\text{GeO}_2$ and $5.5\ \mu\text{m}$ for $\text{SiO}_2+\text{P}_2\text{O}_5$ soot sample. The analytical data are given in details in Table 1. Thus the addition of Ge or P-oxide is found to influence the particle growth dynamics and the viscosity of the silicate, which control the characteristics of the deposited soot network. With the lowering of viscosity, the porous structure fuses together creating larger pores at lower temperatures. The effect is prominent in the case of doping P either in SiO_2 or in a mixture of $\text{SiO}_2+\text{GeO}_2$ soot. The above observations indicate that an SiO_2 layer is most suitable for using as a precursor during solution doping as the network homogeneity and pore size uniformity are superior compared to other compositions. However, experiments reveal that pure SiO_2 deposit has the disadvantage of disengaging during soaking due to poor adhesion with the silica tube surface. So the amount of dopant in the soot deposit and the deposition temperature need to be judiciously selected in order to achieve compositional homogeneity and desired RE concentration in the preform / fiber.

Table 1. Variation of pore sizes with change in composition

Deposition temperature (°C)	Vapor phase composition	Average pore size in μm	Pore area fraction
1250	Pure SiO_2	0.3-0.5	8%
1250	$\text{SiO}_2+\text{GeO}_2$	1.5-2.0	27%
1100	$\text{SiO}_2+\text{P}_2\text{O}_5$	5.0-5.5	50%

The analysis of surface area of the soot particles indicates that the surface area decreases with rise in temperature for the different soot compositions. This is due to partial consolidation of the layer at a higher temperature. The surface area of the pure silica sample is found to be many times higher compared to doped soot samples shown in Table 2. This corresponds to the earlier observation that the doping of GeO_2 or P_2O_5 decreases the viscosity and affects the particle growth. The analysis further indicates that a pure silica soot network will consist of smaller pores compared to silica soot deposit doped with Ge or P. This is also apparent from the image analysis data of the micrograph of deposited layers. Due to higher surface to volume ration in the silica network, the RE concentration in the fabricated fiber is expected to be higher for pure silica deposit compared to Ge or P doped layer if the same solution is used for soaking. The data in Table 2 further show the influence of temperature on the surface area for a specific soot composition. The decrease in temperature by 55°C results in about 2 to 3 times increase in the surface area. Thus the morphology of the soot particles is observed to influence the pore formation and their distribution which control the RE incorporation in the deposit.

Table 2. Surface area of different soot samples

Soot composition	Deposition temperature °C	Surface area, m ² /g
SiO ₂	1200	195.01
	1255	66.79
SiO ₂ +GeO ₂ (GeCl ₄ /SiCl ₄ =0.86)	1200	18.07
	1255	10.32
SiO ₂ +P ₂ O ₅ (POCl ₃ /SiCl ₄ =0.48)	1100	8.8

Chemical analysis of the soot deposit provides an interesting result. It is observed that the GeO₂ proportion in the soot corresponds to about 73% and 81% completion of oxidation reaction of GeCl₄ at core deposition temperatures of 1250°C and 1295°C respectively. The results are quite close to the theoretically calculated conversion of 82% and 87% at the said temperatures. The theoretical analysis was done by considering the reaction as first order with respect to the chloride reactant and evaluating the rate constant values at specific temperatures [17]. The similarity of GeO₂ proportion in the input vapor mixture with that in the unsintered soot layer is very significant as it is directly related to the viscosity of the deposit and extent of sintering at the deposition temperature. The network formation and pore collapsing therefore occur in soot with much higher GeO₂ concentration than that present in the final fiber. A similar result was obtained while analyzing the soot containing P₂O₅. The observation clarifies the significant effect of temperature and composition on the soot layer porosity. Such analysis has not been reported earlier. Usually the GeO₂ incorporation efficiency in the core glass is between 15 to 25% of the vapor phase composition. The present data indicate that the major amount of GeO₂ is lost during sintering and collapsing stages.

Figure 8 is the back scattered electron (BSE) micrograph of the SiO₂+GeO₂ layer shown in Fig. 4(b) after soaking in a solution of 0.01 (M) ErCl₃ + 0.3 (M) AlCl₃ in ethanol for one hour. The solution impregnation through the pores is prominent, with white regions in the picture indicating the presence of higher molecular weight substances like Er (white) and Al (grey). The point that is evident from the soaked layer micrographs is that larger pores draw a greater amount of solution leading to increase in both Al and RE concentration, but act as precursor for development of RE and Al-clusters. While the RE clustering leads to pair induced quenching and degradation in the final fiber performance, the Al clusters are probable sources for Al rich phase separation and defect generation in the core. In this context, pores of smaller sizes are found to be beneficial. However, formation of smaller pores in doped SiO₂ layers by way of partial sintering has the problem of relatively wider variation in pore sizes as already discussed. This increases the probability of non-uniform RE distribution as seen from the Er distribution in Fig. 9, which was measured in the preform sample obtained from the soaked layer shown in Fig. 8. The variation in Er ion concentration at various positions is a consequence of solution impregnation in the pores present in those locations. The pore size variation in the above layer due to deposition at 1295°C has already been described in Fig. 5. The decrease in Er level at the center of the preform is due to evaporation taking place during sintering and collapsing.

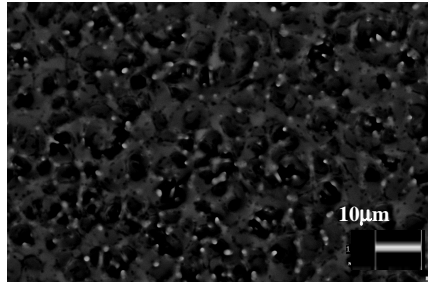


Fig. 8. BSE micrograph of $\text{SiO}_2\text{-GeO}_2$ soot after solution doping.

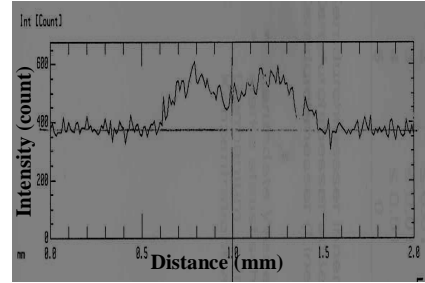


Fig. 9. Radial distribution of Er across the core in the preform.

Table 3 shows the results relating to Er incorporation in three different soot layers deposited with variation in temperature and composition. In fibers F1 and F2, GeO_2 doped core layers were deposited at temperatures of 1255 and 1295°C while in fiber F3, the core was doped with P_2O_5 with the deposition temperature maintained at 1100°C. The solution concentration was same in all the experiments. These are results of three typical preform runs out of a series of runs carried out for such investigation. The absorption at 980 nm in F1 is higher by about 0.90 dB/m in comparison to F2 corresponding to an Er ion concentration difference of 200 ppm. The spectral attenuation curves measured in the fibers are presented in Fig. 10. Thus a concentration difference of 100 ppm is observed for a temperature variation of 20°C for the selected composition. The NA corresponding to this composition was about 0.20. The refractive index profile of the fiber is shown in Fig. 11. The above data is important in order to optimize the solution doping parameters and control the Er concentration in the fiber. Correlating the data with the porous layer morphology, it is observed that partial sintering with collapsing of the pores at higher temperature results in reduced surface to volume ratio and consequently less solution retention in the porous structure, which ultimately leads to lesser incorporation of rare earth ions. The Er concentration obtained in P_2O_5 doped deposit is much higher than that in GeO_2 doped layers. Considering low sintering temperature associated with P doping, it is expected that soot densification will reduce the Er incorporation because of difficulty in solution impregnation. The reverse trend in final Er ion concentration can be explained on the basis of the soot chemistry of Si-P [18] with that of Si-Ge. Substitution of Si by P helps to avoid charge imbalance, which results in additional Al absorption and consequent increases in Er level in the layer. However, from the examination of the soot network structure it appears that P doped layer contains larger pores compared to the Ge doped deposit and has the capacity of retaining a greater amount of solution. This is because in the case of P addition the pores have a tendency to combine together with the disappearance of intermediate walls during partial consolidation instead of mere size reduction.

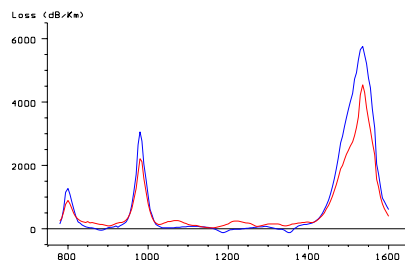


Fig. 10. Spectral attenuation curve of F1 (Blue line) and F2 (Red line) showing Er^{3+} concentration variation.

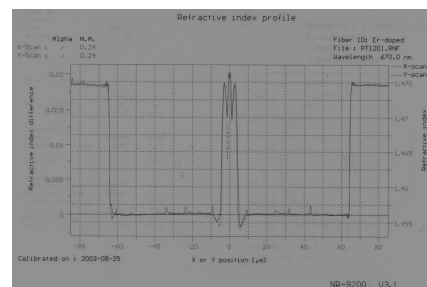


Fig. 11. R.I profile of Fiber F1.

Table 3. Fiber properties and parameters

Fiber	Input vapor mixture	Composition of doping solution used	Deposition temperature, °C	Er ion absorption peak at 980 nm, dB/m	Fiber Characterization	
					NA	Core-diameter in μ
F1	GeCl ₄ /SiCl ₄ =0.86	0.01(M) ErCl ₃ + 0.3(M) AlCl ₃	1255	3.120	0.22	7.6
F2	GeCl ₄ /SiCl ₄ = 0.86	0.01(M) ErCl ₃ + 0.3(M) AlCl ₃	1295	2.265	0.20	7.5
F3	POCl ₃ /SiCl ₄ =0.48	0.01(M) ErCl ₃ + 0.3(M) AlCl ₃	1100	4.990	0.13	6.5

An interesting observation coming out of the above analysis is the relation exhibited by the pore area fraction with the Er ion absorption at 980 nm, which is directly related to the concentration of Er in the core. The absorption of 3.12, 2.27 and 4.99 dB/m (Table 3) is observed against pore area fraction of 32%, 24% and 50% in the porous layer microstructures of fibers F1, F2 and F3 respectively. This corresponds to a relation of $B = c \cdot Q$, where B represents Er ion absorption at 980 nm in dB/m, Q the percent pore area fraction and c is a constant. The value of c is found to be 0.1 for the solution used in the present case. The relation is found to be valid for several fibers fabricated for this purpose. Thus, the factor although empirical, gives a good indication about the final rare earth incorporation in the preform/fiber. Investigation is still continuing to understand the physical significance of the factor. The point that is clear from all the above results is that an analysis of the porous layer microstructures is extremely useful to control the rare earth concentration, distribution and the homogeneity in the final preform/fiber.

4. Conclusion

Investigation of the microstructure of the porous layers deposited by MCVD process shows significant influence of input vapor composition and deposition temperature on the porous network morphology. The compositions selected were SiO₂, SiO₂+GeO₂ and SiO₂+P₂O₅. At higher deposition temperatures the pores collapse and also fuse together leading to reduction in pore size uniformity and decrease in porosity. For GeO₂ doped soot layers, the uniformity reduces from 70% to 59% due to variation in temperature from 1220° to 1295°C. The addition of Ge or P-oxide was found to influence the particle growth dynamics and the viscosity of the silicate, which control the formation of the deposited soot network. With the lowering of viscosity, the porous structure collapses and joins together more easily, creating larger pores even at lower temperatures. Thus the mean pore size is found to be 0.5 μ m for SiO₂, 1.5 μ m for SiO₂+GeO₂ and 5.5 μ m for SiO₂+P₂O₅ soot samples. The surface area of a pure silica sample is about 195 m²/g at 1200°C and several times higher than the doped soot samples. The analysis further indicates that a pure silica soot network consists of smaller pores compared to doped silica soot deposit. Composition analysis of the soot deposit shows that the soot contains a much higher proportion of dopant in comparison to that present in the ultimate core glass. For the SiO₂+GeO₂ layer, the GeO₂ concentration in the soot formed at 1295°C is about 80% of that present in the input vapor. Thus the network formation and pore collapsing occur in soot with much higher GeO₂ or P₂O₅ concentration than that present in the final fiber. The observation explains the significant effect of temperature and composition on the soot layer porosity. The Er concentration and distribution in the final preform/fiber has also been determined with respect to deposition temperature and composition. It is observed that partial sintering with collapsing of the pores at higher temperature results in reduced surface to volume ratio and consequently less solution retention in porous structure, which ultimately

leads to lesser incorporation of rare earth ion. The Er concentration obtained in P₂O₅ doped deposit is much higher than that in GeO₂ doped layers. A pore area fraction, defined on the basis of total pore area compared with the area of the deposit under consideration, is found to explain the rare earth concentration in the preform/fiber. Thus the analysis of the porous layer microstructures is able to provide a quantitative indication of the rare earth incorporation in the deposit and can be a controlling step for fabrication of rare earth doped optical fibers.

Acknowledgments

The authors are thankful to the Director, CG&CRI for his constant encouragement and support in carrying out the investigation. They also like to thank the colleagues of Fiber Optics Laboratory, especially Dr. S.K. Bhadra and K. Dasgupta for their valuable suggestions in the experimental work. Thanks are also due to Dr. Kirchoff of IPHT Jena for extending X-ray microprobe analysis facility. One of the authors Anirban Dhar is thankful to CSIR, India for providing Senior Research Fellowship (SRF).